

ห้องสมุดงานวิจัย สำนักงานคณะกรรมการวิจัยแห่งชาติ



E46924



EFFECTS OF AMBIENT TEMPERATURE ON THE ELASTIC
PROPERTY OF POLYMER GEOGRIDS

MR. WATTIANO TABSOMBUT

A THESIS SUBMITTED IN PARTIAL FULFILLMENT
OF THE REQUIREMENTS FOR
THE DEGREE OF MASTER OF ENGINEERING (CIVIL ENGINEERING)
FACULTY OF ENGINEERING
KING MONKUT'S UNIVERSITY OF TECHNOLOGY THONBURI

2616



E46924

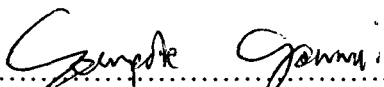
Effects of ambient temperature on the elastic property of polymer geogrids



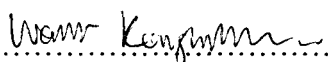
Mr. Watthano Tabsombut B.Eng. (Civil Engineering)

A Thesis Submitted in Partial Fulfillment of the Requirements for
the Degree of Master of Engineering (Civil Engineering)
Faculty of Engineering
King Mongkut's University of Technology Thonburi
2010

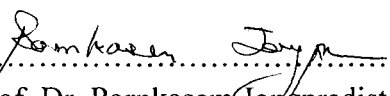
Thesis Committee


.....
(Asst. Prof. Dr. Sompote Youwai, D.Eng.)

Chairman of Thesis Committee


.....
(Asst. Prof. Dr. Warat Kongkitkul, Ph.D.)

Member and Thesis Advisor


.....
(Asst. Prof. Dr. Pornkasem Jongpradist, Ph.D.)

Member and Thesis Co-Advisor


.....
(Lect. Montri Dechasakulsom, Ph.D.)

Member

Thesis Title	Effects of Ambient Temperature on the Elastic Property of Polymer Geogrids
Thesis Credits	12
Candidate	Mr. Watthano Tabsombut
Thesis Advisors	Asst. Prof. Dr. Warat Kongkitkul Asst. Prof. Dr. Pornkasem Jongpradist
Program	Master of Engineering
Field of Study	Civil Engineering (Geotechnical Engineering)
Department	Civil Engineering
Faculty	Engineering
B.E.	2553

E 46924

Abstract

This research is aimed to develop an automated tensile loading system, which can incorporate various loading histories and temperature histories, to determine temperature-dependent elasto-viscoplastic properties of polymer geogrid. A series of Stepped Isothermal Method (SIM) tests, which test specimens were loaded with a constant tensile load while the ambient temperature was stepwise increased, were performed to verify the developed tensile loading system. Then, monotonic loading (ML) tests were performed at different constant temperatures until test specimens rupture to determine the effects of ambient temperature on the tensile strength. In addition, ML tests, which intermission of sustained loading followed by minute-amplitude cyclic loading was performed at different levels of tensile load, were conducted evaluate the elastic property of polymer geogrids. From the test results, it was found that tensile rupture strength of geogrid used in this study decreased significantly with increase of temperature. This result implies that the temperature affects the intrinsic (plastic) stress-strain property of polymer geogrid, which is known to be an elasto-viscoplastic material. The elastic stiffness increased with increase in the load level at fixed temperature, and decreased with increase of the temperature at the same load level. Mathematical expressions are proposed to express these trends of the elastic stiffness described above.

Keywords: Geogrid / Temperature / Tensile Loading Test / Rupture Strength / Elastic Stiffness

หัวข้อวิทยานิพนธ์	ผลกระทบของอุณหภูมิที่มีต่อคุณสมบัติอีลาสติกของจีโอกรีต
หน่วยกิต	12
ผู้เขียน	นายวิฑฒโน ทับสมบัติ
อาจารย์ที่ปรึกษา	ผศ.ดร.วรัช ก้องกิจกุล ผศ.ดร.พรเกษม จงประดิษฐ์
หลักสูตร	วิศวกรรมศาสตรมหาบัณฑิต
สาขาวิชา	วิศวกรรมโยธา (วิศวกรรมเทคนิคธรณี)
ภาควิชา	วิศวกรรมโยธา
คณะ	วิศวกรรมศาสตร์
พ.ศ.	2553

E 46924

บทคัดย่อ

งานวิจัยนี้ เป็นการพัฒนาเครื่องทดสอบแรงดึงซึ่งสามารถควบคุมประวัติการให้แรงและอุณหภูมิ แวดล้อมตัวอย่างได้แบบอัตโนมัติเพื่อศึกษาคุณสมบัติอีลาสโตวิสโคพลาสติกของแผ่นใยสังเคราะห์ โพลีเมอร์ประเภทจีโอกรีต การศึกษาเริ่มจากการเปรียบเทียบเครื่องมือที่ได้พัฒนาโดยการทดสอบการ เร่งการคืบของจีโอกรีตด้วยการให้แรงดึงคงที่กระทำต่อตัวอย่าง ในขณะที่อุณหภูมิแวดล้อมตัวอย่าง ควบคุมให้คงที่และเพิ่มขึ้นในรูปแบบขั้นบันได จากนั้นจึงทดสอบแรงดึงด้วยการให้แรงดึงกระทำ อย่างต่อเนื่องภายใต้อุณหภูมิแวดล้อมตัวอย่างที่แตกต่างกันที่ควบคุมให้คงที่ตลอดการดึงตัวอย่าง จนถึงจุดวิบัติ นอกจากนี้ งานวิจัยนี้ยังได้ทำการทดสอบการดึงตัวอย่างที่แทรกด้วยการให้แรงดึงคงที่ และตามด้วยการให้แรงกระทำเป็นวัฏจักรด้วยแอมพลิจูดขนาดเล็กในระหว่างการดึงตัวอย่างที่ระดับ แรงดึงแตกต่างกัน เพื่อศึกษาคุณสมบัติอีลาสติกของจีโอกรีต ผลการทดสอบพบว่า ค่าแรงดึงสูงสุด ของจีโอกรีตที่ได้ทดสอบในงานวิจัยนี้ มีค่าลดลงอย่างมีนัยเมื่ออุณหภูมิแวดล้อมเพิ่มขึ้น ซึ่งแสดงให้เห็นถึงผลกระทบของอุณหภูมิที่มีต่อคุณสมบัติเนื้อแท้ของจีโอกรีต ซึ่งเป็นวัสดุจำพวกอีลาสโตวิสโค พลาสติก นอกจากนี้ อีลาสติกสตีเฟนสมีค่าเพิ่มขึ้นกับระดับแรงดึง เมื่อพิจารณาที่อุณหภูมิเท่ากัน และ มีค่าลดลงกับอุณหภูมิเมื่อพิจารณาที่ระดับแรงดึงเท่ากัน พฤติกรรมดังกล่าวสามารถสรุปได้เป็น สมการทางคณิตศาสตร์เพื่อใช้ทำนายค่าอีลาสติกสตีเฟนสมือทราบแรงดึงและอุณหภูมิปัจจุบัน

คำสำคัญ: จีโอกรีต / อุณหภูมิ / การทดสอบแรงดึง / กำลังรับแรงดึงสูงสุด / อีลาสติกสตีเฟนส

ACKNOWLEDGEMENTS

The author would like to express his gratitude to his advisor and co-advisor, Asst. Prof. Dr. Warat Kongkitkul and Asst. Prof. Dr. Pornkasem Jongpradist for excellent guidance and strong support throughout his study. Without their help in both academic and personal concerns, this thesis work could not have been completed. Sincere appreciation is also extended to the other members of the committees, Asst. Prof. Dr. Sompote Youwai and Dr. Montri Dechakulsom for their help, encouragement, suggestions, constructive comments and serving as members of his thesis examination committees.

Thanks are also extended to Mr. Thitikorn Posribink, Mr. Bordin Tangcharoensuk and his friends for their kind help and valuable encouragement.

Finally, the author would like to thank his parents and his family for their constant love, strong support and encouragement during studying at King Mongkut's University of Technology Thonburi.

CONTENTS

	PAGE
ENGLISH ABSTRACT	ii
THAI ABSTRACT	iii
ACKNOWLEDGEMENTS	iv
CONTENTS	v
LIST OF TABLES	vii
LIST OF FIGURES	ix
LIST OF SYMBOLS	xix
CHAPTER	
1. INTRODUCTION	1
1.1 State of Problem	1
1.2 Objectives of the Study	1
1.3 Scope and Limitation	2
2. LITERATURE REVIEW	3
2.1 Introduction	3
2.2 Tensile loading test	5
2.3 Current design for geosynthetics	7
2.3.1 Creep reduction factor and creep rupture curve	7
2.3.2 Residual strength curves	12
2.3.2.1 Residual strength curve I	12
2.3.2.2 Residual strength curve II	13
2.3.2.3 Residual strength curve III	18
2.4 Characterization of rapid loading at elevated temperatures	25
2.5 Isochronous theory	27
2.5.1 Introduction of isochronous theory	27
2.5.2 Response of geosynthetic to different loading histories	31
2.6 Elasto-viscoplastic properties	36
2.6.1 General	36
2.6.2 Quantification of viscous properties	42
2.6.3 Elastic properties	45
2.6.4 Stress-strain behavior during cyclic loading	47
2.6.5 Modeling for ageing effects	49
2.6.6 Numerical simulation of temperature-accelerated creep tests	51
3. METHODOLOGY	52
3.1 Introduction	52
3.2 Test materials	52
3.3 Test apparatuses	55
3.3.1 Gripping device	55
3.3.2 Loading system	55
3.3.3 Temperature controlled chamber	55
3.3.4 Heating system and temperature controller	56
3.4 Installation of specimen on the gripping device	59
3.5 Temperature controller operation manual	61

3.5.1	Operation manual	61
3.5.2	Example of programs	63
3.6	Test specimens	64
3.7	Test Programs	66
3.7.1	SIM test	66
3.7.2	Effects of ambient temperature on the elastic property and stress rupture	68
3.8	How to find a current yield point by using radius of curvature, ρ	68
4.	RESULTS AND DISCUSSIONS	69
4.1	Introduction	69
4.2	Stepped Isothermal Method test (SIM test)	69
4.2.1	Introduction	69
4.2.2	Reinforcement 1 (Polypropylene)	70
4.2.3	Reinforcement 2 (High-density polyethylene; HDPE)	85
4.2.4	Reinforcement 3 (Polyester)	100
4.2.5	Comparison between creep rupture curve and creep reduction factor	115
4.3	Effects of temperature on the rupture strength	117
4.3.1	Introduction	117
4.3.2	Continuous monotonic loading test at different temperatures	117
4.3.3	Temperature effect parameter, A'	123
4.4	Effects of temperature on the elastic stiffness	126
4.4.1	Stress-strain relations for minute cyclic loading	126
4.4.2	Equivalent elastic stiffness (k_{eq})	128
4.4.3	Comparison between k_{eq} and temperature	156
5.	CONCLUSIONS	159
	REFERENCES	160
	APPENDICES	
A	Mathematical corrections of the stress rupture and the elastic property and the new reference temperature of 20 °C	163
B	A guide for the generation, manipulation, and presentation of data relating to short term and accelerated creep behavior	171
C	Reducing the viscous effect on small-amplitude unload/reload cycles to determine elastic stiffness by 3-hr creep loading	177
	CURRICULUM VITAE	183

LIST OF TABLES

TABLE	PAGE	
2.1	Typical values of reduction factors in the current design procedures (after Tatsuoka et al., 2004)	11
2.2	Typical values of creep reduction factor (after Tatsuoka et al., 2004)	11
2.3	Reference Tensile Strength Values (after Zornberg et al., 2004)	26
2.4	Two different components of the time effects (modified from Tatsuoka, 2004)	36
2.5	Summary of β -values for respective reinforcements (Kongkitkul, 2004)	44
2.6	List of β -values of geogrids obtained from the literature	44
3.1	Geosynthetic reinforcements used in this study	53
3.2	Panel function in Fig. 3.9	62
3.3	<i>The SET command</i> is used to <i>set</i> values (User level)	63
3.4	Command to open/close a program of temperature controller	63
3.5	Parameters used to set the program on panel function of temperature controller (Fig. 3.9)	67
4.1	Details of the target tensile load and temperature in SIM test on reinforcement 1 (Polypropylene)	70
4.2	Parameters used to scale and shift the test data of reinforcement 1 (Polypropylene)	71
4.3	Details of the target tensile load and temperature in SIM test on reinforcement 2 (High-density polyethylene; HDPE)	85
4.4	Parameters used to scale and shift the test data of reinforcement 2 (High-density polyethylene; HDPE)	86
4.5	Details of the target tensile load and temperature in SIM test on reinforcement 3 (Polyester)	100
4.6	Parameters used to scale and shift the test data of reinforcement 3 (Polyester)	101
4.7	Recommended creep reduction factor (RF_{CR}) values provided in “Designing with Geosynthetics”	115
4.8	Strain rate effect on the rupture tensile strength	119
4.9	Rupture tensile strength obtained by ML test at load rate = 0.6 kN/m/min and different constant temperatures corrected to be the corresponding values at strain rate = 0.1 %/min, for respective reinforcements	120
4.10	β -values used to correct the rupture tensile strength of geogrids obtained from the literature used in the present study	120
4.11	The summary of yield point determined by minimum curvature radius (ρ_{min}) for reinforcement 2 (High-density polyethylene; HDPE)	123
4.12	Constant parameter values in Eq. 4.1 after correction for $\dot{\epsilon} = 0.1$ %/min	124
4.13	Tensile load, V (kN/m) at which small-amplitude cyclic loading (CL) for respective reinforcements	126
4.14	Constant parameters of Eq. 4.3 for respective reinforcements	156
A.1	Rupture tensile strength and temperature effect parameter of the new reference temperature of 20 °C and different constant temperatures corrected to be the corresponding values at strain rate = 0.1 %/min, for respective reinforcements	164

A.2	Constant parameter values in Eq. A.1 after correction for $\dot{\epsilon} = 0.1 \text{ \%}/\text{min}$	165
A.3	Temperature effect parameter of the new reference temperature of 20 °C, $A^{f'}$ and k_{eqo} value and different constant temperatures, for respective reinforcements	168
A.4	Constant parameters of Eq. A.2 for respective reinforcements	169
C.1	Viscous effect parameter ($\epsilon_{cy} / \epsilon_{cr}$) for respective reinforcements	179

LIST OF FIGURES

FIGURE	PAGE
2.1 Schematic creep – rupture curve (after Kongkitkul and Tatsuoka, 2007)	4
2.2 Tensile load-strain relations obtained from monotonic loading tests at different ambient temperature (after Zornberg et al., 2004)	4
2.3 a) Tensile loading apparatus with a pair of roller-clamps and a specimen; and b) a typical ruptured PET geogrid specimen (after Hirakawa et al., 2003)	6
2.4 Rate-dependency of the tensile load-strain behavior (after Hirakawa et al., 2003)	7
2.5 Conventional creep rupture curve (after Greenwood, 1994)	7
2.6 Load-strain relations of geosynthetic reinforcement to obtain conventional creep rupture curve and residual strength curves I (after Tatsuoka et al., 2004)	9
2.7 Conventional creep rupture curve and residual strength curves I for different strain rates (after Tatsuoka et al., 2004)	9
2.8 Design procedure of FHWA to determine the design strength for a given design life (after Tatsuoka et al., 2004)	10
2.9 Loading histories to obtain residual strength curves I (after Tatsuoka et al., 2004)	13
2.10(a) Loading histories to obtain residual strength curves II (in arithmetic scale of time) (after Tatsuoka et al., 2004)	14
2.10(b) Loading histories to obtain residual strength curves II (in logarithm scale of time) (after Tatsuoka et al., 2004)	14
2.11 Load-strain relations of geosynthetic reinforcement to obtain conventional creep rupture curve and residual strength curves II (after Tatsuoka et al., 2004)	15
2.12 Conventional creep rupture curve and residual strength curves I and II (after Tatsuoka et al., 2004)	15
2.13(a) Difference between conventional creep rupture curve and residual strength curve II described in the relation between load and logarithm of time (after Tatsuoka et al., 2004)	17
2.13(b) Difference between conventional creep rupture curve and residual strength curve II described in the relation between strain and time (after Tatsuoka et al., 2004)	17
2.14(a) Load-strain relations of geosynthetic reinforcement to obtain conventional creep rupture curve and residual strength curves III (after Tatsuoka et al., 2004)	19
2.14(b) Difference between loading histories for conventional creep rupture curve and residual strength curve III (after Tatsuoka et al., 2004)	19
2.15 Conventional creep rupture curve and residual strength curve III (after Tatsuoka et al., 2004)	20
2.16 Conventional creep rupture curve and residual strength curves I and III (after Tatsuoka et al., 2004)	20
2.17 Effects of time during SL before the start of ML on the residual strength III (after Tatsuoka et al., 2004)	21

2.18	Residual strength curve proposed by Greenwood, 1994. The residual strength at the design life becomes much greater than the anticipated value from conventional creep rupture curve	22
2.19(a)	Effects of strain rate at rupture on residual strength curves III (after Tatsuoka et al., 2004)	23
2.19(b)	Effects of sustained loading on residual strength curves III (after Tatsuoka et al., 2004)	23
2.20	Difference between the design strength based on creep rupture curve and the actual strength during likely seismic loading (after Tatsuoka et al., 2004)	24
2.21	Effect of temperature on ultimate tensile strength (after Zornberg et al., 2004)	25
2.22(a)	Typical results obtained from the conventional creep tests (after Yeo, 1985)	28
2.22(b)	Isochrones obtained from conventional creep tests in Fig. 2.22a (after Yeo, 1985)	28
2.23(a)	Typical results obtained from CRS tests performed at different but constant strain rate (after Yeo, 1985)	29
2.23(b)	Isochrones obtained from CRS tests in Fig. 2.23a (after Yeo, 1985)	29
2.24	Interpretation of results from ML at different but constant strain rates by isochronous (after Tatsuoka et al., 2004)	30
2.25	Proposed loading histories to examine the relevance of isochronous theory (after Tatsuoka et al., 2004)	30
2.26(a)	Tensile load-strain relation upon the restart of loading at point <i>b</i> according to isochronous theory (after Tatsuoka et al., 2004)	32
2.26(b)	Tensile load-strain relation upon the restart of loading at point <i>f</i> (the end of sustained loading <i>e-f</i> in test 3) according to isochronous theory (after Tatsuoka et al., 2004)	32
2.26(c)	Comparison of load-strain relation from tests 2 and 3 according to isochronous theory (after Tatsuoka et al., 2004)	33
2.27(a)	Actual response of geosynthetic reinforcement to different loading histories (after Tatsuoka et al., 2004)	34
2.27(b)	Actual response of geosynthetic reinforcement upon the restart of loading at point <i>f</i> (the end of sustained loading <i>e-f</i> in test 3) (after Tatsuoka et al., 2004)	34
2.27(c)	Actual response of geosynthetic reinforcement from tests 2 and 3 (after Tatsuoka et al., 2004)	35
2.28	a) Elasto-plastic material; b) various loading histories with a single stress variable; and c) response (Tatsuoka, 2007).	36
2.29	a) Non-linear three-component model (Di Benedetto et al., 2002; Tatsuoka et al., 2002); and b) stress parameters relevant to unbound geomaterials and the stress path in drained TC (σ_{ij} indicates the stress vector) (Tatsuoka et al., 2007)	38
2.30	Four basic viscosity types of geomaterials in shear and definitions of rate-sensitivity coefficients, β & $\beta_{residual}$ (Tatsuoka, 2007)	38
2.31	a) FE mesh for a GRS-RW model; and b) measured average vertical footing pressure-footing settlement relation and its FE simulation (after Noguchi et al., 2006)	41

2.32	Definitions of tensile load jump a) step increase without decay; b) step decrease without decay; c) step increase with decay; and d) step decrease with decay (after Hirakawa, 2003)	42
2.33	Load jump plotted against load corresponding to stepwise changes in the strain rate, reinforcement 8 (V-3000) (Kongkitkul, 2004)	43
2.34	Relation between $\Delta V/V$ and logarithm of strain rate ratios, reinforcement 8 (V-3000) (Kongkitkul, 2004)	44
2.35	Definitions of equivalent elastic stiffness, k_{eq}	45
2.36	Evaluation of elastic properties, reinforcement 8 (V-3000) (Kongkitkul, 2004)	45
2.37	Relationships between equivalent elastic stiffness and load level, reinforcement 8 (V-3000) (Kongkitkul, 2004)	46
2.38	Response of: a) an elasto-plastic material free from both inviscid cyclic loading effect and ageing effect; and b) an elasto- <i>viscoplastic</i> material free from both inviscid cyclic loading effect and ageing effect (after Tatsuoka, 2006)	47
2.39	Response of; a) an elasto-plastic material with significant inviscid cyclic loading effect while free from ageing effect: and b) an elasto- <i>viscoplastic</i> material with significant inviscid cyclic loading effect while free from ageing effect (after Tatsuoka, 2006)	48
2.40	Yield inviscid tensile load increment V_y^f developed by increments of irreversible strain and time when both viscous and ageing effects are active (after Tatsuoka et al., 2003, 2008)	50
2.41	Numerical simulated results for SIM test at tensile load equal to 40 kN/m: a) tensile load-strain relation; and b) time history of tensile strain (after Kongkitkul and Tatsuoka, 2007)	51
3.1	Dimensional characteristic of geosynthetic reinforcements	53
3.2	Specimen installed with the gripping device and the frame measurement of deformation for: a) reinforcement 1 (Polypropylene); b) reinforcement 2 (High-density polyethylene; HDPE); and c) reinforcement 3 (Polyester)	54
3.3	Temperature-controlled and load rate-controlled tensile loading apparatus	56
3.4	Schematic diagram of the all test apparatus	57
3.5	Schematic diagram of the flow of hot air in the chamber	57
3.6	Calibration of the maximum difference temperature installed thermometers at many locations inside the chamber	58
3.7	A typical time history of measured temperature inside the temperature-controlled chamber	58
3.8(a)	Fasten a specimen to the lower clamp by using a small steel rod (after Hirakawa, 2003)	60
3.8(b)	Wrap a specimen around the lower clamp (after Hirakawa, 2003)	60
3.8(c)	Wrap a specimen around the upper clamp (after Hirakawa, 2003)	60
3.8(d)	Fasten a specimen to the upper clamp by using a small steel rod (after Hirakawa, 2003)	60
3.9	Panel function of temperature controller	61
3.10	Example of process temperature controller	64
3.11(a)	Front view details of the specimen set up and a LVDT installed for local axial deformation measurement	65
3.11(b)	Side view details of the specimen set up and a LVDT installed for local axial deformation measurement	65

4.1	Relationships between the tensile load (V) and the modulus and the tensile strain, for reinforcement 1 (Polypropylene)	71
4.2	Relationships between the tensile load (V) and the creep strain and the elapsed time during creep, for reinforcement 1 (Polypropylene)	72
4.3	Relationships between the tensile load (V) and the creep modulus and the elapsed time during creep, for reinforcement 1 (Polypropylene)	72
4.4	Time histories of tensile strain at: a) $V= 54.3$ kN/m; and b) $V= 58.6$ kN/m, for reinforcement 1 (Polypropylene)	73
4.4	Time histories of tensile strain at: c) $V= 62.9$ kN/m, for reinforcement 1 (Polypropylene)	74
4.5	Time (log-scale) histories of creep strain at different temperatures during SL after rescaling at: a) $V= 54.3$ kN/m; and b) $V= 58.6$ kN/m, for reinforcement 1 (Polypropylene)	75
4.5	Time (log-scale) histories of creep strain at different temperatures during SL after rescaling at: c) $V= 62.9$ kN/m, for reinforcement 1 (Polypropylene)	76
4.6	Time (log-scale) histories of creep modulus at different temperatures during SL after rescaling at: a) $V= 54.3$ kN/m; and b) $V= 58.6$ kN/m, for reinforcement 1 (Polypropylene)	77
4.6	Time (log-scale) histories of creep modulus at different temperatures during SL after rescaling at c) $V= 62.9$ kN/m, for reinforcement 1 (Polypropylene)	78
4.7	Time (log-scale) histories of creep strain at: a) $V= 54.3$ kN/m; and b) $V= 58.6$ kN/m, for reinforcement 1 (Polypropylene) (after removing the initial non-linear part and vertical shifting of the curves presented in Figures 4.5a and 4.5b)	79
4.7	Time (log-scale) histories of creep strain at: c) $V= 62.9$ kN/m, for reinforcement 1 (Polypropylene) (after removing the initial non-linear part and vertical shifting of the curves presented in Figure 4.5c)	80
4.8	Time (log-scale) histories of creep modulus at: a) $V= 54.3$ kN/m; and b) $V= 58.6$ kN/m, for reinforcement 1 (Polypropylene) (after removing the initial non-linear part and vertical shifting of the curves presented in Figures 4.6a and 4.6b)	81
4.8	Time (log-scale) histories of creep modulus at: c) $V= 62.9$ kN/m, for reinforcement 1 (Polypropylene) (after removing the initial non-linear part and vertical shifting of the curves presented in Figures 4.6c)	82
4.9	Master curves in terms of: a) creep strain; and b) creep modulus, for reinforcement 1 (Polypropylene)	83
4.10	Creep–rupture curves in terms of: a) tensile load; and b) percentage of tensile load, for reinforcement 1 (Polypropylene)	84
4.11	Relationships between the tensile load (V) and the modulus and the tensile strain, for reinforcement 2 (High-density polyethylene; HDPE)	86
4.12	Relationships between the tensile load (V) and the creep strain and the elapsed time during creep, for reinforcement 2 (High-density polyethylene; HDPE)	87
4.13	Relationships between the tensile load (V) and the creep modulus and the elapsed time during creep, for reinforcement 2 (High-density polyethylene; HDPE)	87

4.14	Time histories of tensile strain at: a) $V= 53.9$ kN/m; and b) $V= 59.2$ kN/m, for reinforcement 2 (High-density polyethylene; HDPE)	88
4.14	Time histories of tensile strain at: c) $V= 64.6$ kN/m, for reinforcement 2 (High-density polyethylene; HDPE)	89
4.15	Time (log-scale) histories of creep strain at different temperatures during SL after rescaling at: a) $V= 53.9$ kN/m; and b) $V= 59.2$ kN/m, for reinforcement 2 (High-density polyethylene; HDPE)	90
4.15	Time (log-scale) histories of creep strain at different temperatures during SL after rescaling at: c) $V= 64.6$ kN/m, for reinforcement 2 (High-density polyethylene; HDPE)	91
4.16	Time (log-scale) histories of creep modulus at different temperatures during SL after rescaling at: a) $V= 53.9$ kN/m; and b) $V= 59.2$ kN/m, for reinforcement 2 (High-density polyethylene; HDPE)	92
4.16	Time (log-scale) histories of creep modulus at different temperatures during SL after rescaling at: c) $V= 64.6$ kN/m, for reinforcement 2 (High-density polyethylene; HDPE)	93
4.17	Time (log-scale) histories of creep strain at: a) $V= 53.9$ kN/m; and b) $V= 59.2$ kN/m, for reinforcement 2 (High-density polyethylene; HDPE) (after removing the initial non-linear part and vertical shifting of the curves presented in Figures 4.15a and 4.15b)	94
4.17	Time (log-scale) histories of creep strain at: c) $V= 64.6$ kN/m, for reinforcement 2 (High-density polyethylene; HDPE) (after removing the initial non-linear part and vertical shifting of the curves presented in Figure 4.15c)	95
4.18	Time (log-scale) histories of creep modulus at: a) $V= 53.9$ kN/m; and b) $V= 59.2$ kN/m, for reinforcement 2 (High-density polyethylene; HDPE) (after removing the initial non-linear part and vertical shifting of the curves presented in Figures 4.16a and 4.16b)	96
4.18	Time (log-scale) histories of creep modulus at: c) $V= 64.6$ kN/m, for reinforcement 2 (High-density polyethylene; HDPE) (after removing the initial non-linear part and vertical shifting of the curves presented in Figures 4.16c)	97
4.19	Master curves in terms of: a) creep strain; and b) creep modulus, for reinforcement 2 (High-density polyethylene; HDPE)	98
4.20	Creep–rupture curves in terms of: a) tensile load; and b) percentage of tensile load, for reinforcement 2 (High-density polyethylene; HDPE)	99
4.21	Relationships between the tensile load (V) and the modulus and the tensile strain, for reinforcement 3 (Polyester)	101
4.22	Relationships between the tensile load (V) and the creep strain and the elapsed time during creep, for reinforcement 3 (Polyester)	102
4.23	Relationships between the tensile load (V) and the creep modulus and the elapsed time during creep, for reinforcement 3 (Polyester)	102
4.24	Time histories of tensile strain at: a) $V= 42.7$ kN/m; and b) $V= 45.8$ kN/m, for reinforcement 3 (Polyester)	103
4.24	Time histories of tensile strain at: c) $V= 49.0$ kN/m, for reinforcement 3 (Polyester)	104
4.25	Time (log-scale) histories of creep strain at different temperatures during SL after rescaling at: a) $V= 42.7$ kN/m; and b) $V= 45.8$ kN/m, for reinforcement 3 (Polyester)	105

4.25	Time (log-scale) histories of creep strain at different temperatures during SL after rescaling at: c) $V= 49.0$ kN/m, for reinforcement 3 (Polyester)	106
4.26	Time (log-scale) histories of creep modulus at different temperatures during SL after rescaling at: a) $V= 42.7$ kN/m; and b) $V= 45.8$ kN/m, for reinforcement 3 (Polyester)	107
4.26	Time (log-scale) histories of creep modulus at different temperatures during SL after rescaling at: c) $V= 49.0$ kN/m, for reinforcement 3 (Polyester)	108
4.27	Time (log-scale) histories of creep strain at: a) $V= 42.7$ kN/m; and b) $V= 45.8$ kN/m, for reinforcement 3 (Polyester) (after removing the initial non-linear part and vertical shifting of the curves presented in Figures 4.25a and 4.25b)	109
4.27	Time (log-scale) histories of creep strain at: c) $V= 49.0$ kN/m, for reinforcement 3 (Polyester) (after removing the initial non-linear part and vertical shifting of the curves presented in Figure 4.25c)	110
4.28	Time (log-scale) histories of creep modulus at: a) $V= 42.7$ kN/m; and b) $V= 45.8$ kN/m, for reinforcement 3 (Polyester) (after removing the initial non-linear part and vertical shifting of the curves presented in Figures 4.26a and 4.26b)	111
4.28	Time (log-scale) histories of creep modulus at: c) $V= 49.0$ kN/m, for reinforcement 3 (Polyester) (after removing the initial non-linear part and vertical shifting of the curves presented in Figures 4.26c)	112
4.29	Master curves in terms of: a) creep strain; and b) creep modulus, for reinforcement 3 (Polyester)	113
4.30	Creep–rupture curves in terms of percentage of tensile load for: a) reinforcement 1 (Polypropylene); and b) reinforcement 2 (High-density polyethylene; HDPE)	116
4.31	Tensile load – strain relations obtained from continuous ML tests until rupture at different constant ambient temperatures, for reinforcement 1 (Polypropylene)	117
4.32	Tensile load – strain relations obtained from continuous ML tests until rupture at different constant ambient temperatures, for reinforcement 2 (High-density polyethylene; HDPE)	118
4.33	Tensile load – strain relations obtained from continuous ML tests until rupture at different constant ambient temperatures, for reinforcement 3 (Polyester)	118
4.34	Method to determine yield point by plot curvature radius and strain relation of curve fitted to the tensile load – strain relations (full-log) obtained from ML at temperature (T) of: a) 30 °C; and b) 35 °C, for reinforcement 2 (High-density polyethylene; HDPE)	121
4.34	Method to determine yield point by plot curvature radius and strain relation of curve fitted to the tensile load – strain relations (full-log) obtained from ML at temperature (T) of: c) 40 °C; and d) 45 °C, for reinforcement 2 (High-density polyethylene; HDPE)	122
4.34	Method to determine yield point by plot curvature radius and strain relation of curve fitted to the tensile load – strain relations (full-log) obtained from ML at temperature (T) of: e) 50 °C, for reinforcement 2 (High-density polyethylene; HDPE)	123

4.35	Temperature effect parameter A' as a function of temperature, T , for reinforcement 1 (Polypropylene)	124
4.36	Temperature effect parameter A' as a function of temperature, T , for reinforcement 2 (High-density polyethylene; HDPE)	125
4.37	Temperature effect parameter A' as a function of temperature, T , for reinforcement 3 (Polyester)	125
4.38	Tensile load – strain relations obtained from ML with small-amplitude unload/reload cycles at various tensile load levels under different constant temperatures, for reinforcement 1 (Polypropylene)	126
4.39	Tensile load – strain relations obtained from ML with small-amplitude unload/reload cycles at various tensile load levels under different constant temperatures, for reinforcement 2 (High-density polyethylene; HDPE)	127
4.40	Tensile load – strain relations obtained from ML with small-amplitude unload/reload cycles at various tensile load levels under different constant temperatures, for reinforcement 3 (Polyester)	127
4.41	Determinations of equivalent stiffness (k_{eq}) from unloading branches of small-amplitude unload/reload cycles at temperature (T) of 30 °C and load level (V/V_{max}) of: a) 0.161; and b) 0.322, for reinforcement 1 (Polypropylene)	128
4.41	Determinations of equivalent stiffness (k_{eq}) from unloading branches of small-amplitude unload/reload cycles at temperature (T) of 30 °C and load level (V/V_{max}) of: c) 0.483; and d) 0.645, for reinforcement 1 (Polypropylene)	129
4.42	Determinations of equivalent stiffness (k_{eq}) from unloading branches of small-amplitude unload/reload cycles at temperature (T) of 35 °C and load level (V/V_{max}) of: a) 0.166; and b) 0.332, for reinforcement 1 (Polypropylene)	130
4.42	Determinations of equivalent stiffness (k_{eq}) from unloading branches of small-amplitude unload/reload cycles at temperature (T) of 35 °C and load level (V/V_{max}) of: c) 0.498; and d) 0.664, for reinforcement 1 (Polypropylene)	131
4.43	Determinations of equivalent stiffness (k_{eq}) from unloading branches of small-amplitude unload/reload cycles at temperature (T) of 40 °C and load level (V/V_{max}) of: a) 0.170; and b) 0.341, for reinforcement 1 (Polypropylene)	132
4.43	Determinations of equivalent stiffness (k_{eq}) from unloading branches of small-amplitude unload/reload cycles at temperature (T) of 40 °C and load level (V/V_{max}) of: c) 0.511; and d) 0.682, for reinforcement 1 (Polypropylene)	133
4.44	Determinations of equivalent stiffness (k_{eq}) from unloading branches of small-amplitude unload/reload cycles at temperature (T) of 45 °C and load level (V/V_{max}) of: a) 0.174; and b) 0.347, for reinforcement 1 (Polypropylene)	134
4.44	Determinations of equivalent stiffness (k_{eq}) from unloading branches of small-amplitude unload/reload cycles at temperature (T) of 45 °C and load level (V/V_{max}) of: c) 0.521; and d) 0.694, for reinforcement 1 (Polypropylene)	135

4.45	Determinations of equivalent stiffness (k_{eq}) from unloading branches of small-amplitude unload/reload cycles at temperature (T) of 50 °C and load level (V/V_{max}) of: a) 0.177; and b) 0.355, for reinforcement 1 (Polypropylene)	136
4.45	Determinations of equivalent stiffness (k_{eq}) from unloading branches of small-amplitude unload/reload cycles at temperature (T) of 50 °C and load level (V/V_{max}) of: c) 0.532, for reinforcement 1 (Polypropylene)	137
4.46	Determinations of equivalent stiffness (k_{eq}) from unloading branches of small-amplitude unload/reload cycles at temperature (T) of 30 °C and load level (V/V_{max}) of: a) 0.151; and b) 0.302, for reinforcement 2	138
4.46	Determinations of equivalent stiffness (k_{eq}) from unloading branches of small-amplitude unload/reload cycles at temperature (T) of 30 °C and load level (V/V_{max}) of: c) 0.453; and d) 0.603, for reinforcement 2 (High-density polyethylene; HDPE)	139
4.47	Determinations of equivalent stiffness (k_{eq}) from unloading branches of small-amplitude unload/reload cycles at temperature (T) of 35 °C and load level (V/V_{max}) of: a) 0.159; and b) 0.318, for reinforcement 2 (High-density polyethylene; HDPE)	140
4.47	Determinations of equivalent stiffness (k_{eq}) from unloading branches of small-amplitude unload/reload cycles at temperature (T) of 35 °C and load level (V/V_{max}) of: c) 0.478; and d) 0.637, for reinforcement 2 (High-density polyethylene; HDPE)	141
4.48	Determinations of equivalent stiffness (k_{eq}) from unloading branches of small-amplitude unload/reload cycles at temperature (T) of 40 °C and load level (V/V_{max}) of: a) 0.174; and b) 0.348, for reinforcement 2 (High-density polyethylene; HDPE)	142
4.48	Determinations of equivalent stiffness (k_{eq}) from unloading branches of small-amplitude unload/reload cycles at temperature (T) of 40 °C and load level (V/V_{max}) of: c) 0.522; and d) 0.696, for reinforcement 2 (High-density polyethylene; HDPE)	143
4.49	Determinations of equivalent stiffness (k_{eq}) from unloading branches of small-amplitude unload/reload cycles at temperature (T) of 45 °C and load level (V/V_{max}) of: a) 0.193; and b) 0.386, for reinforcement 2 (High-density polyethylene; HDPE)	144
4.49	Determinations of equivalent stiffness (k_{eq}) from unloading branches of small-amplitude unload/reload cycles at temperature (T) of 45 °C and load level (V/V_{max}) of: c) 0.580; and d) 0.773, for reinforcement 2 (High-density polyethylene; HDPE)	145
4.50	Determinations of equivalent stiffness (k_{eq}) from unloading branches of small-amplitude unload/reload cycles at temperature (T) of 50 °C and load level (V/V_{max}) of: a) 0.206; and b) 0.411, for reinforcement 2 (High-density polyethylene; HDPE)	146
4.50	Determinations of equivalent stiffness (k_{eq}) from unloading branches of small-amplitude unload/reload cycles at temperature (T) of 50 °C and load level (V/V_{max}) of: c) 0.617; and d) 0.823, for reinforcement 2 (High-density polyethylene; HDPE)	147
4.51	Determinations of equivalent stiffness (k_{eq}) from unloading branches of small-amplitude unload/reload cycles at temperature (T) of 30 °C and load level (V/V_{max}) of: a) 0.118; and b) 0.235, for reinforcement 3 (Polyester)	148

4.51	Determinations of equivalent stiffness (k_{eq}) from unloading branches of small-amplitude unload/reload cycles at temperature (T) of 30 °C and load level (V/V_{max}) of: c) 0.353; and d) 0.470, for reinforcement 3 (Polyester)	149
4.52	Determinations of equivalent stiffness (k_{eq}) from unloading branches of small-amplitude unload/reload cycles at temperature (T) of 40 °C and load level (V/V_{max}) of: a) 0.121; and b) 0.242, for reinforcement 3 (Polyester)	150
4.52	Determinations of equivalent stiffness (k_{eq}) from unloading branches of small-amplitude unload/reload cycles at temperature (T) of 40 °C and load level (V/V_{max}) of: c) 0.363; and d) 0.484, for reinforcement 3 (Polyester)	151
4.53	Determinations of equivalent stiffness (k_{eq}) from unloading branches of small-amplitude unload/reload cycles at temperature (T) of 50 °C and load level (V/V_{max}) of: a) 0.247; and b) 0.370, for reinforcement 3 (Polyester)	152
4.53	Determinations of equivalent stiffness (k_{eq}) from unloading branches of small-amplitude unload/reload cycles at temperature (T) of 50 °C and load level (V/V_{max}) of: c) 0.493, for reinforcement 3 (Polyester)	153
4.54	Relationships between equivalent stiffness and normalized tensile load level at different temperatures, for reinforcement 1 (Polypropylene)	154
4.55	Relationships between equivalent stiffness and normalized tensile load level at different temperatures, for reinforcement 2 (HDPE)	154
4.56	Relationships between equivalent stiffness and normalized tensile load level at different temperatures, for reinforcement 3 (Polyester)	155
4.57	Relationship between k_{eqo} (Eq. 4.2) and parameter A' of Eq. 4.1 with respective temperatures, for reinforcement 1 (Polypropylene)	157
4.58	Relationship between k_{eqo} (Eq. 4.2) and parameter A' of Eq. 4.1 with respective temperatures, for reinforcement 2 (HDPE)	157
4.59	Relationship between k_{eqo} (Eq. 4.2) and parameter A' of Eq. 4.1 with respective temperatures, for reinforcement 3 (Polyester)	158
A.1	Temperature effect parameter of the new reference temperature of 20 °C, A'' as a function of temperature, T , for reinforcement 1 (Polypropylene)	166
A.2	Temperature effect parameter of the new reference temperature of 20 °C, A'' as a function of temperature, T , for reinforcement 2 (High-density polyethylene; HDPE)	166
A.3	Temperature effect parameter of the new reference temperature of 20 °C, A'' as a function of temperature, T , for reinforcement 3 (Polyester)	167
A.4	Relationship between k_{eqo} (Eq. 4.2) and parameter A'' of Eq. A.1 with respective temperatures, for reinforcement 1 (Polypropylene)	169
A.5	Relationship between k_{eqo} (Eq. 4.2) and parameter A'' of Eq. A.1 with respective temperatures, for reinforcement 2 (HDPE)	170
A.6	Relationship between k_{eqo} (Eq. 4.2) and parameter A'' of Eq. A.1 with respective temperatures, for reinforcement 3 (Polyester)	170
B.1	Creep versus time at various loadings	173
B.2	Curve fitted creep curves	174
B.3	Sherby-Dorn plot	174
B.4	Isochronous load-strain curves	175

B.5	Boltzmann principle applied to creep curve with increasing loadings	175
B.6	Creep curve @ σ_3 loading	176
C.1	Time histories of tensile strain increment on ten small-amplitude unload/reload cycles, ε_{cy} and 3-hr creep loading, ε_{cr} at temperature (T) of 50 °C and load level (V/V_{max}) of 0.174, for reinforcement 1 (Polypropylene)	180
C.2	Viscous effects on small-amplitude unload/reload cycles after 3-hr creep loading at temperature (T) of 50 °C and load level (V/V_{max}) of: a) 0.174; and b) 0.348, for reinforcement 1 (Polypropylene)	181
C.2	Viscous effects on small-amplitude unload/reload cycles after 3-hr creep loading at temperature (T) of 50 °C and load level (V/V_{max}) of: c) 0.521; and d) 0.695, for reinforcement 1 (Polypropylene)	182

LIST OF SYMBOLS

A'	=	temperature effect parameter
CL	=	cyclic loading
HDPE	=	High-Density Polyethylene
k_{eq}	=	equivalent stiffness
k_{eqo}	=	equivalent stiffness at rupture tensile strength
LVDT	=	Linear variable displacement transducer
ML	=	monotonic loading
MD	=	machine direction (longitudinal to the roll)
PET	=	Polyester
PP	=	Polypropylene
RF_{CR}	=	creep reduction factor
RF_D	=	durability reduction factor
RF_{ID}	=	installation damage factor
SIM	=	Stepped Isothermal Method
SL	=	sustained loading
t	=	time
T	=	temperatures
T_o	=	reference temperature (30 °C)
TD	=	transverse directions (across roll width)
TTS	=	Time-Temperature Superposition
V	=	tensile load
V_{max}	=	rupture tensile strength
V_{maxo}	=	rupture strength obtained from a monotonic loading test at reference temperature (30 °C)
V_{ult}	=	ultimate tensile strength
V_y	=	yield tensile strength
ρ	=	radius of curvature
β	=	rate-sensitivity coefficient
$\beta_{residual}$	=	residual rate-sensitivity coefficient
ε	=	tensile strain
$\dot{\varepsilon}$	=	strain rate